

Simulations of a neutral complex (OH^- , H_3O^+)

Abstract

In recent years, molecular dynamics simulations on water-based deep eutectic solvents (DES) have increased. Most of these studies highlight the fact that to faithfully reproduce the dynamic properties of the latter using an atomic force field (TIP3P, COSMO, SPC / E and model 1) at a fixed charge, it is necessary to resort to updating the scale of the load. In this work, we propose an alternative to the scaling of the charges on the complex (OH^- , H_3O^+) and show that the only refinement of the LENNARD-JONES parameters of oxygen of the hydroxyl function in TIP3P and SPC / E allows an accurate description of the static, dynamic and structural property parameters of two commonly used DES. Various physicochemical properties calculated for mixtures with our modified version of TIP3P and SPC / E are in good agreement with the experimental data. Finally, the calculated radial distribution functions correspond to those reported in the literature.

Keywords: Water; the hydrogen bond; model ; molecular dynamics.

1. Introduction

Water is the most abundant solvent in nature. It plays an important role in several chemical and biological processes. Various physical properties of water, such as density, dielectric constant, compressibility etc, are well established. Besides this, water has many unusual properties such as high dielectric constant, negative volume of melting, numerous crystalline polymorphs, anomalously high melting and high mobility transport for H^+ and OH^- ions, boiling and critical temperatures for a low-molecular-weight substance etc. Such properties can be explained in the light of the formation of three-dimensional water-water hydrogen bonding networks.

Further, it has been found that the structural and dynamic properties of biomolecules are highly dependent on the solvent, such as the water surrounding them. These waters are popularly known as “biological water [1].

The main theoretical approaches to address these questions are quantum mechanics (QM) and molecular dynamics (MD), respectively. Dynamic Car-Parrinello simulations based on the DFT representation of the potential energy can combine both approaches but remain limited to relatively small systems.

The motivation for this work lies in the fact that elucidating the key design differences between the hydroxide (OH^-) and hydronium (H_3O^+) diffusion mechanisms will play an important role in the discovery and determination of key design principles for the synthesis of new membrane materials with high ion conductivity for the use in emerging fuel cell technologies this end, ab initio molecular dynamics simulations (AIMD) are presented to explore (OH^- , H_3O^+) solvation complexes and diffusion mechanisms in the model1, TIP3P, COSOM and SPC / E systems at hydration in confined environments. The two systems were first equilibrated at room temperature using a massive Nosé–Hoover chain thermostat, followed by 0–1000 ps of canonical (NVT) dynamics, Dispersion forces were accounted for using the Dispersion-Corrected Atomic Core Pseudopotential (DCACP) scheme within the Kohn–Sham formulation of Density Functional Theory using the B-LYP exchange-correlation functional. The B-LYP+DCACP has been selected for this study, as it has previously been shown to produce satisfactory results for water-acene interactions [2], liquid water [3],

The studies here involve a single ($\text{OH}^- \dots \text{H}_3\text{O}^+$) pair in a water box with (H_3O^+) counterions, corresponding to a concentration of about 0.01 mol/l. Further investigations are being pursued:

- (i) First, the effect of aqueous concentration by simulating a more concentrated solution (about 0.1 mol/l)
- (ii) we want to evaluate to what extent the results of model 1 were satisfied with respect to the models (TIP3P, COSOM, SPC/E) of the (OH^- , H_3O^+)(H_2O)_n complex.

2. Materials and methods

The systems were simulated by classical molecular dynamics “MD” using the modified AMBER.10 software [4] in which the potential energy U is described empirically by a sum of the bond, angle and dihedral strain energies and one additive per pair 1-6-12 (electrostatic + van der Waals) interactions between unbound atoms.

$$U = \sum_{\text{bonds}} K_r (r - r_{\text{eq}})^2 + \sum_{\text{angles}} K_\theta (\theta - \theta_{\text{eq}})^2 + \sum_{\text{dihedrals}} \sum_n V_n (1 + \cos n\phi) + \sum_{i < j} 4\epsilon_{ij} \left(\left(\frac{R_{ij}^0}{R_{ij}} \right)^{12} - \left(\frac{R_{ij}^0}{R_{ij}} \right)^6 \right) + \sum_i q_i q_j / R_{ij} - C / R_{ij}^6$$

Cross terms in van der Waals interactions were constructed using Lorentz-Berthelot rules. The parameters of the (H_3O^+) and (OH^-) ions were taken from references [5], respectively, and the (H_3O^+) charges were adjusted to the electrostatic potentials (DFT-B3LYP / 6-31G ** calculations). For the solvent, we used the TIP3P model [6] for water [7]. We also tested the SPC / E model [8] of water for the solution, (OH^- , H_3O^+)(H_2O)₂₅₆

All the simulations were performed at 300K with periodic boundary conditions in a cubic box with a side length of 5 Å. Each box contained 256 water molecules. The systems were first minimized using the conjugate gradient energy minimization method. Then, gradually, the temperature of each system was increased to the room temperature of 300 K within a short MD run. This was carried out at constant pressure ($P=1$ atm) under the isothermal-isobaric ensemble (NPT) conditions. It was then followed by an NPT equilibration run at 300 K for 10 ns duration for each of the systems. The temperature and pressure of the systems were controlled by Langevin dynamics and Nose–Hoover Langevin piston methods.

The cell volumes were allowed to fluctuate isotropically during this period. At the end of these NPT runs, the volumes of the system attained steady values with cell edge lengths 39.68, 39.48

and 39.65 Å for simulations. The dimensions of the simulation cells were then fixed, and the conditions were changed to constant temperature (300 K) and volume (NVT ensemble) after 10 ns. MD time step of 1 fs was used to integrate the equations of motion via the leapfrog algorithm. was employed for each of the simulations, and the trajectories were stored every 1000 fs for subsequent analysis.

3. Results

3.1. Temperature and energy

The temperature and energy of the four simulation models (TIP3P, COSMO, SPC / E and model 1) are carried out. We have presented only Model 1. It is clear, that during the equilibration period, there are fluctuations in temperature and energy values, which is expected. Further, it can be seen that during the production run, the temperature of the four systems remains constant. The energy of the systems also achieved almost steady value. This indicates that the systems are well-balanced.

3.2. (OH^- , H_3O^+) $(\text{H}_2\text{O})_{256}$ Structure

In this work, we have calculated $g(r)$ between the oxygen atoms O-O of the ions. The calculations were carried out for all three models (TIP3P, SPC / E and model 1), and the results were compared with experimental data. The calculations were carried out by taking the average of all oxygen atoms of ions, and the result is displayed in Figure (1). We did not take into consideration the COSOM model because it presents a larger volume of O-O of 20% compared to the TIP3P model, according to the literature.

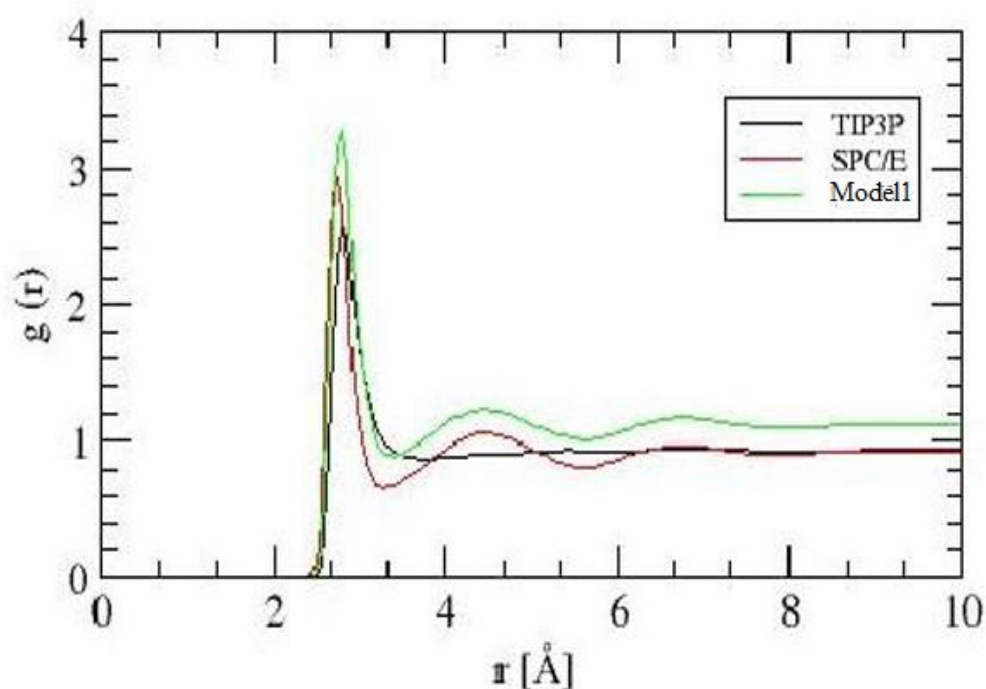


Figure (1). Pairwise correlation function, $g(r)$, of ions for all three models.

For all three models, there is a sharp first peak. The first peak for TIP3P ,SPC/E and Model 1 appears at around 2.8 Å, 2.7 Å and 2.6 Å respectively. The first peak is followed by a second peak at around 4.6 Å for the modèle 1 and SPC/E model. Beyond that, the structure of the ion almost disappears except for the modèle 1. Further, among the three models, the modèle 1 shows a highly intense first peak, which is followed by second and third peaks of low intensity, indicating the highest structuring of the modèle 1 as compared to the other two models TIP3P ,SPC/E . The highest structuring of the modèle 1 may be due to the formation of a larger number of intermolecular hydrogen bonds than the other two models TIP3P ,SPC/E. The values are shown in TABLE (I).

TABLE (I): Parameters of TIP3P, SPC/E ,COSOM and Model1 (^-OH , H_3O^+)

Parameters	TIP3P	SPC/E	COSOM	Model 1
r_{oo} (Å°)	2.80	2.80	2.08	2.08
σ_{oo} (Å°)	5	5	5	5
r_{OH} (Å°)	0.98	0.98	0.98	0.98
HOH angle	110.02	110.02	110.02	110.02
$q_{i(e)}$	-0.83	-0.83	-0.83	-0.83
$q_{j(e)}$	0.417	0.417	0.417	0.417
C_{ij}	-	-	-	8210.2

3.3. Translational Motion

T

he translational motion of ions was studied from the simulated trajectories by calculating the mean-square-displacements (MSD) $\langle \Delta r^2 \rangle$ of ions. The MSD can be defined as,

$$\langle \Delta r^2 \rangle = \langle |r_i(t) - r_i(0)|^2 \rangle$$

where the $r_i(t)$ and $r_i(0)$ are the position vectors of the oxygen atom of the i th ion molecule at time t and at $t = 0$, respectively.

The averaging is carried out over all ion-lead at different time origins. The calculations are carried out for the four models. The values are shown in Table (II).

TABLE (II). Self-Diffusion co-efficient, D ($10^{-9} \text{ m}^2 \text{ s}^{-1}$) values of TIP3P, SPC/E, MOSOM and model 1. The experimental D value for ion-water has also been included in the table for comparison.

Systems	Self diffusion co-efficients (D)water	Self diffusion co-efficients (D) H_3O^+	Self diffusion co-efficients (D) OH^-
TIP4P	3.8	-	-
SPC/E	2.8	-	-
MOSOM	2.5	0.09	0.35
Model 1	2.7	0.07	0.13
OH^- [32]	0.17	-	0.45
Water (experiment) ^{9,10}	2.3	-	-

We have compared the values with experimentally available data and found that among the four models (TIP3P, SPC/E, MOSOM and model 1), the self-diffusion coefficient value for COSOM and Model 1 ion-waters are well correlated with the experimental value.

4. Discussion

The first solvation envelope of oxygen hydroxide (OH^-) is located at 2.7 \AA , as was previously shown for the overall solution [11,12,13,14,15,16,17,18,19] and contains two water oxygens and one hydronium ion (H_3O^+) (instead of three). Oxygens of water as was observed in the overall solution). The CN of the second solvation shell (located $\sim 4 \text{ \AA}$ into the bulk solution [11,12,13,14,15,16,17,18,19]) the second solvation shell of two water oxygens contains eight oxygens. It is well known that the diffusion mechanism of hydroxide ions (OH^-) is strongly affected by the solvation structure of OH^- [11,12,13,14,15,16,17,18,19].

While in bulk solution, the hydroxide ions (OH^-) typically share similar solvation patterns, which results in a similar diffusion mechanism in this low-hydration model 1, the heterogeneity of the environments of each hydroxide (OH^-) suggests that over the time scales of the simulations, each OH^- might be governed by different diffusion mechanisms, The hydroxide ion (OH^-) and the two water molecules continue to diffuse by vehicular diffusion toward the neighboring cation until the hydroxide ion (OH^-) forms, once again, the stable, “at rest” triple structure near the next cation.

The first solvation shell of the hydronium ion (H_3O^+) is located at 2.6 Å. In order to better understand the conditions that allow the diffusion of hydronium ions (H_3O^+), indicated, the first peak, located at ~ 4.2 Å, corresponds to H_3O^+ in which an H_3O^+ has transferred a proton to an OH^- , while the second peak is located at ~ 3.7 Å. The values for the first and second solvation layers are 2.7 and 4.2, respectively. This suggests that, following the following reaction: $\text{OH}^- + \text{H}_3\text{O}^+ \leftrightarrow \text{H}_2\text{O} + \text{H}_2\text{O}$, a neutral species exists in the system. To verify this, we calculate the percentage of time hydronium ions (H_3O^+) spend as OH^- and H_2O , which shows that the hydronium ion (H_3O^+) appears as H_2O for 48.78% of the simulation time.

This leads us to conclude that the protonation state of the system (OH^- , H_3O^+) is an important factor in the diffusion mechanism of hydronium ions (H_3O^+) because the reaction: $\text{OH}^- + \text{H}_3\text{O}^+ \leftrightarrow \text{H}_2\text{O} + \text{H}_2\text{O}$ is a key element in the process of diffusion. The first peak is located at 2.7 Å, and the CN values for the first and second solvation are 4.2 Å $^\circ$, respectively. First, the hydronium ion (H_3O^+) is located in the center of the cell, solvated by two water molecules and a hydroxide ion (OH^-).

In the present work, we used Model 1 and MOSOM simulations to obtain an in-depth atomistic perspective of two models, SPC/E and idealized in confined geometries under hydration conditions ($\lambda = 10$ and 1000). We found that for both systems, the distribution of water within the simulation cell is not uniform. However, the effect of this unique water distribution on the diffusion mechanisms of hydroxide (OH^-) and hydronium (H_3O^+) is fundamentally different. Hydroxide ions have both a first and a second solvation shell; the diffusion mechanism is mainly vehicular [20]. However, the diffusion of hydronium ions (H_3O^+) is structural rather than vehicular, with the participation of anions according to the reaction: $\text{OH}^- + \text{H}_3\text{O}^+ \leftrightarrow \text{H}_2\text{O} + \text{H}_2\text{O}$ see Figure (2).

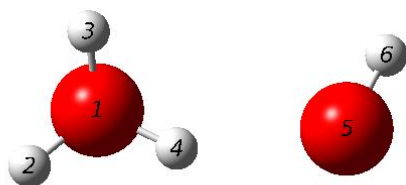


Figure (2). The structure (OH^- , H_3O^+).

Comparing water diffusion, we find that for model 1, the diffusion coefficients of hydroxide ions (OH^-) and water molecules are similar because vehicular diffusion requires synchronized

diffusion of both species. However, for the TIP3P, SPC/E model, water molecules diffuse much more slowly than hydronium ions (H_3O^+), suggesting that water mobility is not necessarily required in the structural diffusion process of hydronium ions.

In this work, we have identified the fundamental atomistic steps governing the transport phenomena of hydroxide (OH^-) and hydronium (H_3O^+). We find that hydroxide (OH^-) diffusion is mostly vehicular, while hydronium (H_3O^+) diffusion is structural.

The results presented show that the OH^- ions diffuse only when they have a second solvation shell of at least one water oxygen. The second solvation shell provides the necessary hydration that is required for the OH^- to shift the competition between its hydrophobic repulsion from the cation and its electrostatic attraction to the cation, which results in vehicular diffusion. Hence, we find that the presence of a second solvation shell promotes vehicular diffusion.

Using AIMD simulations, we have been able to provide atomistic insight, gaining a fundamental understanding of the uniqueness of hydroxide (OH^-) and hydronium ion (H_3O^+) solvation patterns and diffusion mechanisms in this hitherto unstudied regime.

5. Conclusion:

In this work, we used Model 1 with other models (TIP3P, COSMO, SPC/E), the latter of which are well referenced in the literature. For Model 1, the diffusion coefficients of hydroxide ions (OH^-) and water molecules are similar, as vehicular diffusion requires synchronized diffusion of both species. However, for the TIP3P and SPC/E models, water molecules diffuse much more slowly than hydronium ions (H_3O^+), suggesting that water mobility is not necessarily required in the structural diffusion process of hydronium ions (H_3O^+). We concluded that hydroxide (OH^-) diffusion is primarily vehicular, while hydronium (H_3O^+) diffusion is structural. From this research, we identified the fundamental atomistic steps governing hydroxide (OH^-) and hydronium (H_3O^+) transport phenomena.

8. Reference :

- [1] Kamat,(2002) P.V. Photophysical, Photochemical and Photocatalytic Aspects of Metal Nanoparticles. *Journal of Physical Chemistry B*, (**106**), 7729-7744.
- [2]S. Murad, D.J Evans, K.E Gubbins, W.B Street, D.J Tildesley, (1979) *Mol. Phys.* (**37**), 725 .<https://doi.org/10.1080/00268977900103151>
- [3] L . M . Sesé, Feynman-Hibbs (1994) potentials and path integrals for quantum Lennard-Jones systems: theory and Monte-Carlo simulation. *Molec Phys*,1(**312**) 81-1297, 1312 .DOI:[10.1080/00268979500101571](https://doi.org/10.1080/00268979500101571)
- [4] J . S . Rowlinson and al (1969), *Liquids and Liquid Mixtures*. 2nd ed.(Butterworths). London,, **51**..
- [5]F.Benyettou,S.Hiadi and A.Bendraoua (2013),*Oriental.J.Chem.*,Vol.29(**2**),483-490. DOI:[10.13005/ojc/290212](https://doi.org/10.13005/ojc/290212)
- [6] *Cryogenic Fuels*(1991) Liquid Methane Fuel Characterization and Safety Assessment Report. Cryogenic Furt No. CFI-1600.
- [7] S. Nosé,(1984)*J. Chem.Phys.* **81**, 511 .<https://doi.org/10.1063/1.447334>
- [8]F. Belkacem. A. Krallafa, (2005).*J. Soc. Chem. Phys. Alg.* **1**, 15
- [9]Price, W. S.; Ide, H.; Arata, Y. (.1999) *J. Phys. Chem. A* **103**, 448 .
- [10]Ma, Z.; Tuckerman, M.E. (**2011**) On the connection between proton transport, structural diffusion, and reorientation of the hydrated hydroxide ion as a function of temperature.*Chem.Phys.Lett.*,511,177-182
<https://doi.org/10.1016/j.cplett.2011.05.066>
- [11]Tuckerman, M.; Laasonen, K.; Sprik, M.; Parrinello, M. (**1995**)Ab Initio Molecular Dynamics Simulation of the Solvation and Transport of H₃O⁺ and OH⁻ Ions in Water. *J. Phys. Chem.* , **99**, 5749–5752
<https://doi.org/10.1021/j100016a003>
- [12] Marx, D.; Tuckerman, M.E.; Hutter, J.; Parrinello, M.(**1995**) The nature of the hydrated excess proton in water. *Nat. Cell Biol*, **397**, 601–604.
- [13] Tuckerman, M.E.; Marx, D.; Parrinello, M. (**2002**) The nature and transport mechanism of hydrated hydroxide ions in aqueous solution. *Nat. Cell Biol.* , **417**, 925–929 DOI: [10.1038/nature00797](https://doi.org/10.1038/nature00797)
- [14] Tuckerman, M.E.; Chandra, A.; Marx, D. (**2006**) Structure and Dynamics of OH⁻(aq). *Acc. Chem. Res.*, **39**, 151–158 DOI: [10.1021/ar040207n](https://doi.org/10.1021/ar040207n)
- [15] Chandra, A.; Tuckerman, M.E.; Marx, D. (**2007**) Connecting Solvation Shell Structure to Proton Transport Kinetics in Hydrogen-Bonded Networks via Population Correlation Functions. *Phys. Rev. Lett.*, **99**, 145901 . DOI: <https://doi.org/10.1103/PhysRevLett.99.145901>
- [16] Marx, D.; Chandra, A.; Tuckerman, M.E. (**2010**).Aqueous Basic Solutions: Hydroxide Solvation, Structural Diffusion, and Comparison to the Hydrated Proton. *Chem. Rev.* , **110**, 2174–2216 DOI: [10.1021/cr900233f](https://doi.org/10.1021/cr900233f)
- [17] Ma, Z.; Tuckerman, M.E. (**2011**)On the connection between proton transport, structural diffusion, and reorientation of the hydrated hydroxide ion as a function of temperature. *Chem. Phys. Lett.*, **511**, 177–182 <https://doi.org/10.1016/j.cplett.2011.05.066>
- [18] Tuckerman, M.E.; Chandra, A.; Marx, D. A (**2010**) Statistical Mechanical Theory of Proton Transport Kinetics in Hydrogen-Bonded Networks Based on Population Correlation Functions with Applications to Acids and Bases. *J. Chem. Phys.***133**, 124108–124129 . DOI:[10.1063/1.3474625](https://doi.org/10.1063/1.3474625)
- [19] Hassanali, A.; Giberti, F.; Cuny, J.; Kühne, T.D.; Parrinello, M. (**2013**)..Proton transfer through the water gossamer. *Proc. Natl. Acad. Sci. USA*, **110**, 13723–13728
<https://doi.org/10.1073/pnas.1306642110>
-

[20] Tuckerman, M.E.; Marx, D.; Parrinello, M. (2002) The nature and transport mechanism of hydrated hydroxide ions in aqueous solution. *Nat. Cell Biol*, **417**, 925–929 DOI: [10.1038/nature00797](https://doi.org/10.1038/nature00797)
